RESPONSES OF A GLOBAL CGCM TO CO_2 INCREASE

LI Qingquan (李清泉)

National Climate Center, Beijing 100081

and *Scott B. POWER*

Bureau of Meteorology Research Centre, Melbourne, Australia

Received December 28, 1998; revised August 12, 1999

ABSTRACT

The responses of the climate system to increase of atmospheric carbon dioxide (CO_2) are studied by using a new version of the Bureau of Meteorological Research Centre (BMRC) global coupled general circulation model (CGCM). Two simulations are run: one with atmospheric CO_2 concentration held constant at 330 ppm, the other with a tripling of atmospheric CO_2 (990 ppm). Results from the 41-year control coupled integration are applied to analyze the mean state, seasonal cycle and interannual variability in the model. Comparisons between the greenhouse experiment and the control experiment then provide estimations of the influence of increased CO_2 on climate changes and climate variability. Especially discussed is the question on whether the climate changes concerned with CO_2 increase will impact interannual variability in tropical Pacific, such as ENSO.

Key words: CGCM, carbon dioxide, climate change, ENSO

I. INTRODUCTION

Presently, global warming has been a main topic of climate changes. Carbon dioxide (CO_2) is the most important greenhouse gas that increases atmospheric concentration due to human activities. Scientists have already noted to simulate the impacts of CO_2 increase on climate of earth by using various kinds of atmospheric general circulation models coupled with various kinds of oceanic models. Those oceanic models are from assuming SST and sea ice equal to observations to simple swamp models (see Gates et al. 1981; Washington and Meehl 1986), and from intermediate mixed layer oceanic models (see Schlesinger and Zhao 1989) to more complicated and better general circulation oceanic models (see Meehl et al. 1993; Knutson et al. 1997). In previous studies on climate changes related to CO_2, CO_2 concentrations were mostly increased at a constant percent or doubled the initial level, and less attention was paid to the relationship between CO_2 increase and ENSO. In this paper, the CO_2 level was raised to three times of its mid-1980s level (i.e. from 330 ppm to 990 ppm). The BMRC (Bureau of Meteorology Research Centre) coupled atmosphere-ocean-ice dynamic model is used to analyze systematically the climate changes resulting from the increased CO_2. Particularly, questions on ENSO and CO_2-induced global warming are discussed. For example, will the CO_2 increase make ENSO occur more frequently? Will ENSO become stronger? The model and experiment

design are described in Section II. In Section III. the climatological characteristics of control experiment ($1CO_2$ experiment) are compared with those of observation. The differences between greenhouse experiment ($3CO_2$ experiment) and control experiment ($1CO_2$ experiment) are examined in Section IV. The last part. Section V. is summary and concluding remarks.

II. DESCRIPTION OF MODEL AND EXPERIMENT

The model used here is a new version of BMRC coupled general circulation model (CGCM). The atmospheric component is a R21/L9 version of the BMRC atmospheric general circulation model (AGCM). Rhomboidal truncation occurs at wave number 21. Meridional and zonal resolutions are 5. 6° and 3. 2° respectively. "Sigma" coordinates are used in the vertical direction, with 9 unequally spaced levels. The oceanic component is a global version of the GFDL modular ocean model (MOM). There are 25 vertical levels, with the maximum depth being 5000 m. The zonal grid spacing is 2° and the meridional grid spacing ranges from 0. 5° near equator to 5. 85° near pole. The sea ice model is a version of Semtner-type "zero-layer" thermodynamic model. It is a simple model with uniform thickness of sea ice. The zonal and meridional resolutions of the sea ice model are the same as those of the atmospheric model. Because the resolutions and grids of the oceanic model differ from those of the atmospheric and sea ice model. interpolation becomes an important issue of coupling atmospheric model with oceanic model. Translation of variables (e. g. . unit changes. grid rotations. interpolation etc.) is done in separate routines to enhance modularity. The atmospheric, oceanic and sea-ice components are all driven by a small main program. The AGCM was integrated for 3. 5 years using observational SSTs prior to coupling.

In the present paper, two experiments were conducted. In the control run. the coupled model was integrated for 41 years with the CO_2 level of atmospheric model fixed at mid-1980s level of 330 ppm. In the sensitivity run. the CO_2 level of atmospheric model was increased three-fold during the first year and then integrated for a further 40 years. This gives the model a chance to adjust to the new value. We will refer to the control run as the $1CO_2$ run and the sensitivity run as the $3CO_2$ run. The results of the last 20 years in the greenhouse experiment were then compared with the results of the corresponding period in the control experiment to estimate the impacts of increased CO_2 on the earth's climate for a CO_2 tripling.

III. COMPARISON OF THE $1CO_2$ AND OBSERVED CLIMATES

In this section. the results from the last 20 years (year 22—41) of the 41-year control integration are used to compare the simulated $1CO_2$ climate with the observed climate in order to assess the strength and weakness of the CGCM used here.

As a result. the model precipitation is overall reasonably good (Fig. 1). Over Northern America. Southeast Asia and the area extending eastward along 10°N and 10°S. the precipitation is greatest. These features represent the model Inter-Tropical Convergence Zone (ITCZ) and Southern Pacific Convergence Zone (SPCZ). But compared with observation. the model ITCZ is a little too far north. and the model SPCZ is too zonal

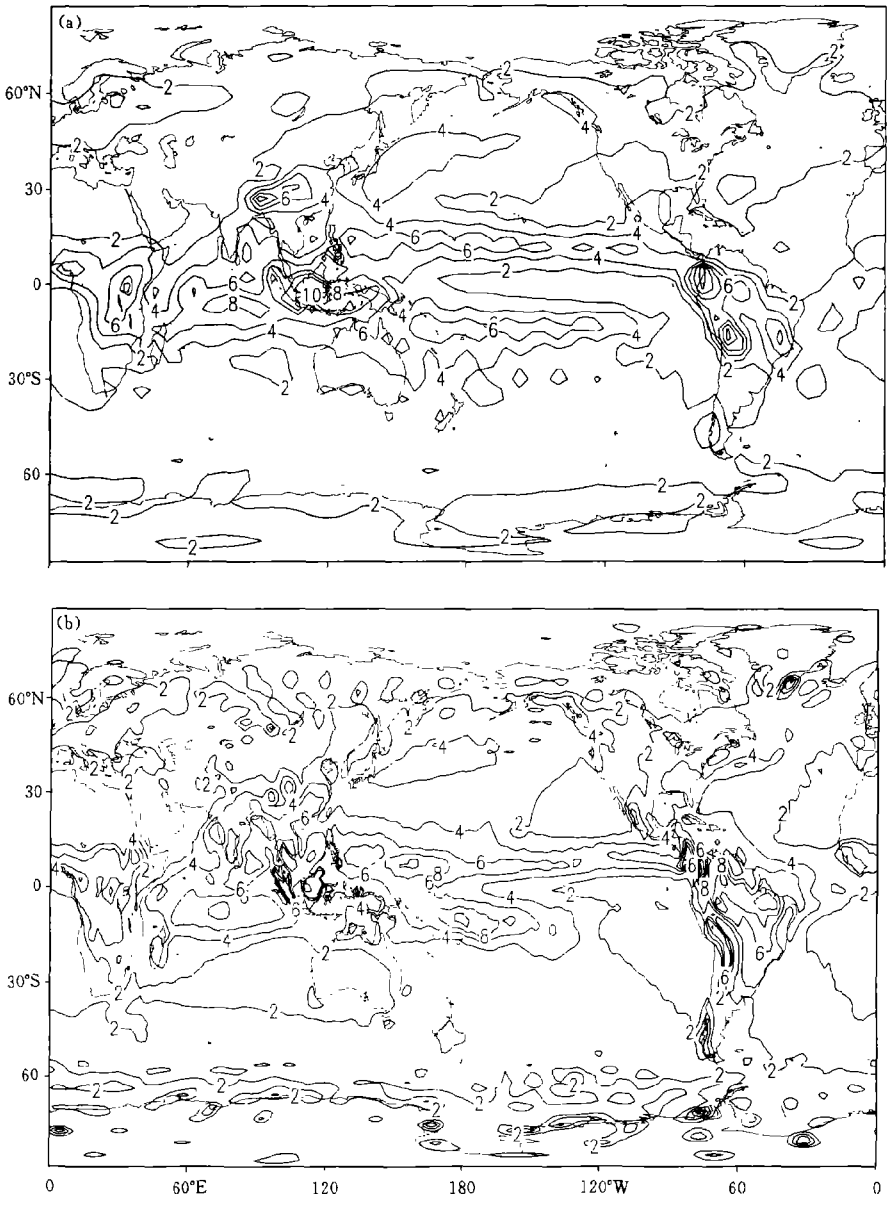

Fig. 1. Annual mean precipitation. (a) Averaged over the last 20 years (year 22—41) of the control run, and (b) averaged from 1979 to 1995 with NCEP reanalysis data (unit: mm d^{-1}).

in orientation.

In the Pacific Ocean, the highest SSTs are located in the west, with coolest SSTs in the central and eastern Pacific, which is same as observation (Fig. 2). But the cold water tongue extends too far west and splits the warm pool, resulting in SSTs in the western Pacific too low along the equator. The seasonal cycle of SST averaged over 5°N—5°S along

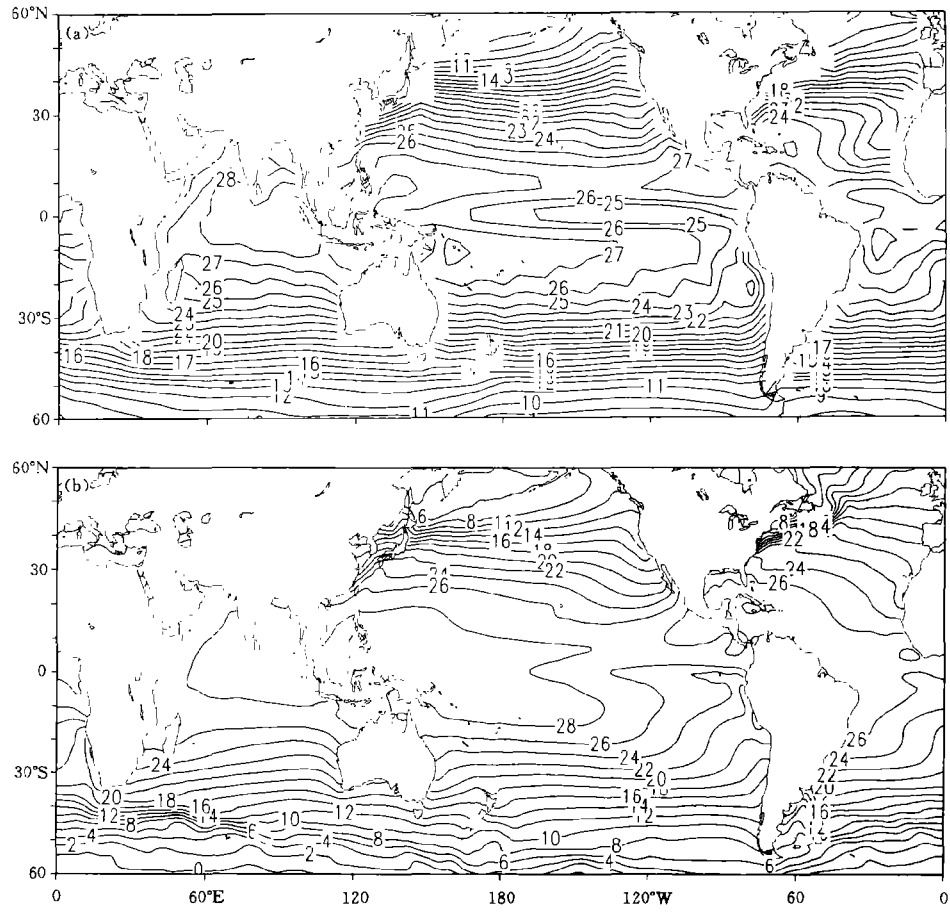

Fig. 2. Annual mean sea surface temperature. (a) Averaged over the last 20 years (year 22—41) of the control run, and (b) averaged from 1979 to 1995 with NCEP reanalysis data (unit: °C).

the equator is similar to observation, but the lowest model SST in the eastern equatorial Pacific (26.5°C, near 150°E) in April—May differs from observation (29°C, near 170°E) in March (figure not shown). However, as it is observed, the simulated interannual variability of SST is largest in the eastern equatorial Pacific Ocean (see Fig. 3). But the level of variability is smaller than observation. Actually, it is a common problem met with by other models (e.g. Meehl et al. 1993; Knutson et al. 1997; Tett 1995).

IV. COMPARISON OF THE $3CO_2$ AND $1CO_2$ CLIMATES

In this section, we compare the simulated $3CO_2$ climate with the $1CO_2$ climate to assess the CO_2-induced climate changes. A tripling CO_2 rather than the more conventional doubling CO_2 is chosen to enhance the signal-to-noise ratio. We hope to address some interesting and important possibilities.

1. *Global and Hemispheric Means*

Table 1 presents the differences between annual means of eight selected quantities in

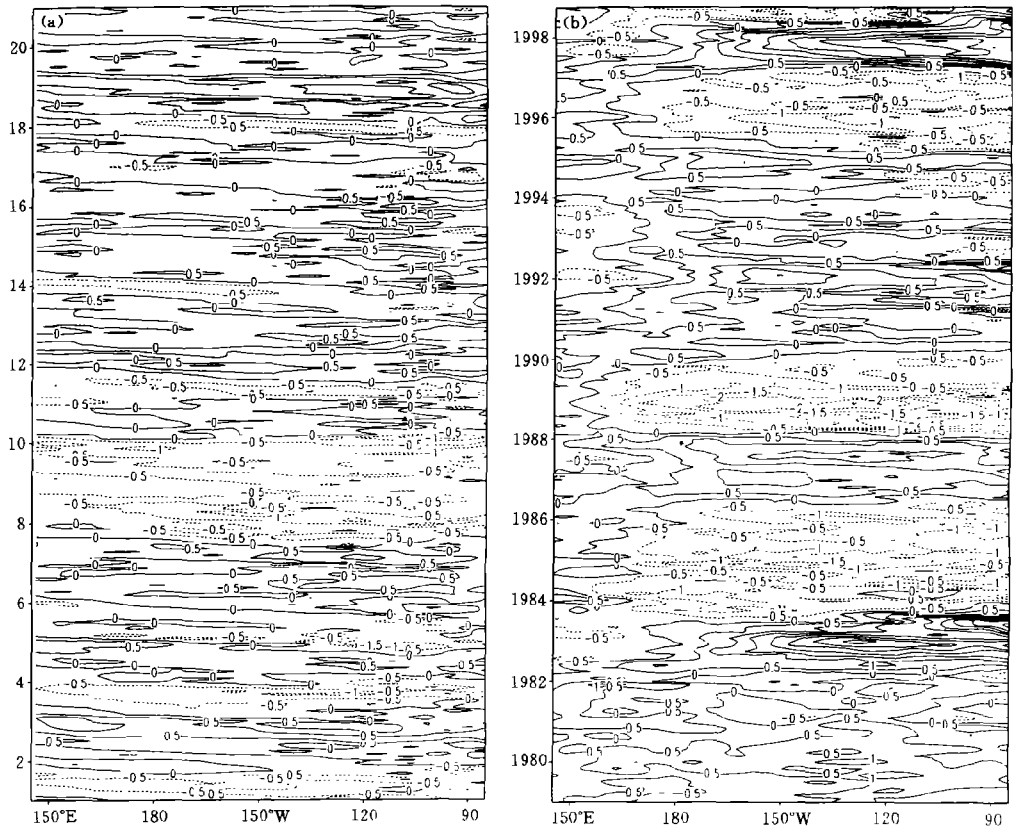

Fig. 3. The longitude-time section of sea surface temperature anomaly over Pacific along equator (5°N − 5°S). (a) Averaged over the last 20 years (year 22 − 41) of the control run, and (b) averaged from 1979 to 1987 with Climate Analysis Center data and from 1982 to 1998 with National Center for Environmental Prediction reanalysis data (unit: °C).

Table 1. Differences of $3CO_2$ Minus $1CO_2$ Annual Mean Eight Quantities Averaged over Globe and Hemisphere

	SST ℃	LST ℃	TSF ℃	DTMAX ℃	DTMIN ℃	PREC mm/d	SM cm	SLP hPa
global mean	2.07	3.82	2.94	2.88	3.12	0.10	−0.39	−0.49
NH mean	1.87	4.14	3.31	3.19	3.58	0.08	−0.45	−0.55
SH mean	2.17	3.37	2.57	2.58	2.67	0.11	−0.12	−0.44

Note: SST: sea surface temperature, LST: land surface temperature, TSF: surface (ocean and land) temperature, DTMAX: daily maximum temperature, DTMIN: daily minimum temperature, PREC: precipitation rate, SM: soil moisture, SLP: sea level pressure.

$3CO_2$ level with those in $1CO_2$ level averaged over globe and hemisphere. Due to the increase of greenhouse effect, both global mean and hemisphere mean temperatures (mean surface temperature, sea surface temperature, land surface temperature, daily maximum temperature, daily minimum temperature) and precipitation increase but mean sea level pressure and mean soil moisture decrease. The rise of mean temperature results mainly from the rising of daily minimum temperature. Daily minimum temperature increases more than daily maximum temperature, and the temperature rises more significantly in land than in ocean. The alteration of SST in the Southern Hemisphere (SH) is larger than that in the Northern Hemisphere (NH) and the mean surface temperature and land surface temperature increase in NH much more than in SH. The change of soil moisture in NH is 0.33 cm larger than that in SH, while the increase of precipitation in SH is 0.31 cm d^{-1} larger than that in NH. The increase of precipitation is associated with the enhancement of hybrid cycle discovered by other greenhouse researches (see Houghton 1994).

As shown in Table 2, the global warming computed under $3CO_2$ condition in this paper is 2.94°C, which is 0.39°C and 1.64°C higher than those computed under $2CO_2$ condition with GFDL model (2.55°C) and NCAR model (1.30°C) respectively. The global mean precipitation rate increases 3.74%, which is about half of the precipitation of NCAR's 9.29%. The decrease of soil moisture (−0.39 cm) is consistent with the simulation of GFDL (−0.21 cm), but opposite to the simulation of NCAR (0.0791 cm) (see Li and Zhao 1996).

Table 2. Comparisons with Simulations of Other Models

Model	BMRC	NCAR	GFDL
CO_2 concentration	$3CO_2$	$2CO_2$	$2CO_2$
Global mean temperature	2.94°C	1.30°C	2.55°C
Global mean precipitation	3.74%	9.29%	——
Global mean soil moisture	−0.39 cm	0.0791 cm	−0.21 cm

In the report in 1990, IPCC indicates that the "best" estimation of increase of global mean temperature is 2.5°C under the condition that the current CO_2 concentration is doubled. It is also pointed out that estimation of global warming is impossible out of the range from 1.5 to 4.5 ℃ (see Houghton 1994). Therefore, the estimation 2.94°C here is in the range of IPCC's estimation.

2. *Zonal Means and Geographic Distributions*

Zonal mean results (Fig. 4) demonstrate that sea surface temperature and total (ocean and land) surface temperature rise at all latitudes, precipitation rate increases at all latitudes except for two regions near 25°N and 45°N. The difference between $3CO_2$ simulation and $1CO_2$ simulation shows that the rising of sea surface temperature and surface (ocean and land) temperature is smaller in tropics, but increases with latitude increasing. The variation of zonally averaged soil moisture is positive in the regions near

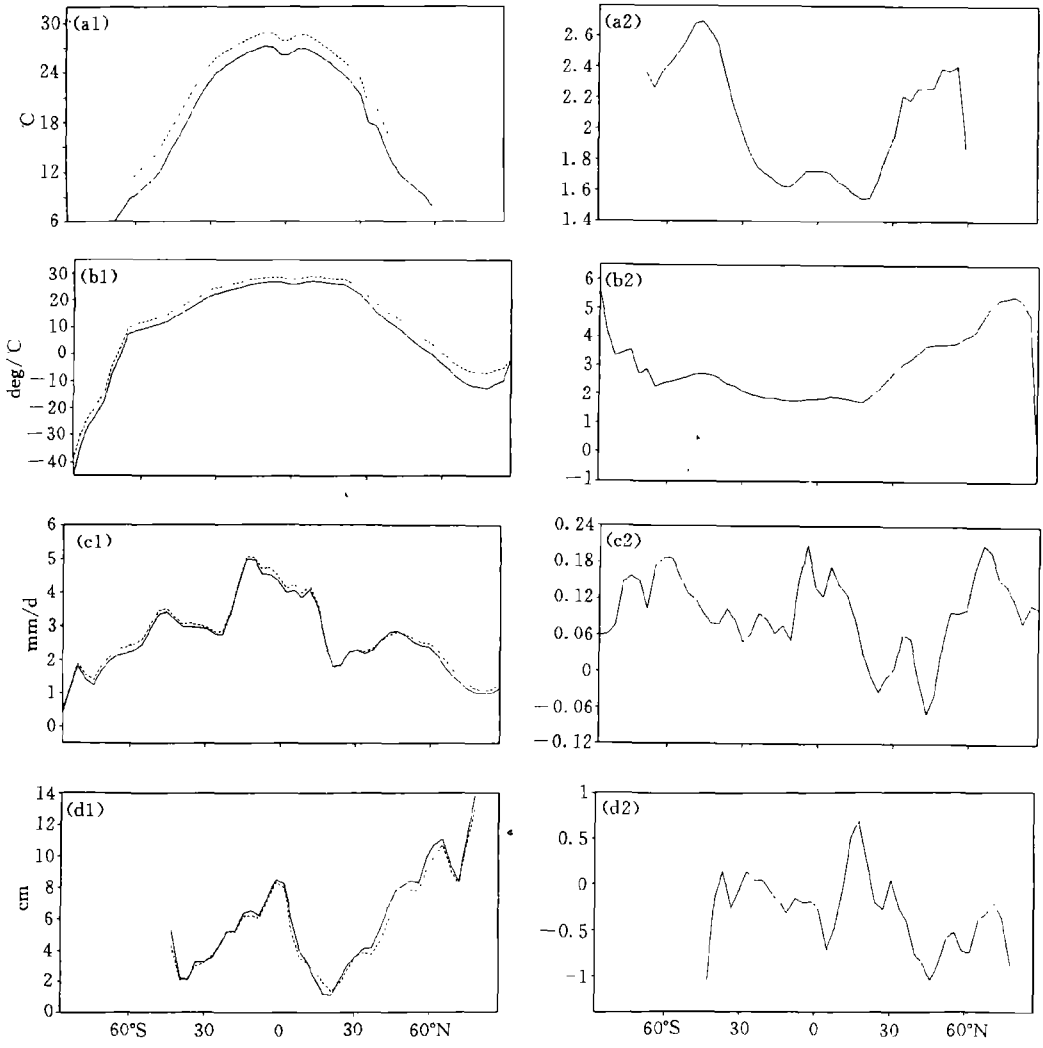

Fig. 4. Zonally averaged annual mean sea surface temperature (Figs. a1 and a2), surface (ocean and land) temperature (Figs. b1 and b2), precipitation rate (Figs. c1 and c2) and soil moisture (Figs. d1 and d2). The left-hand panels of figures show zonal means of each quantity in $1CO_2$ level (solid curve) and $3CO_2$ level (dash curve), the right-hand panels of figures show zonal means of $3CO_2$ minus $1CO_2$ differences of each quantity.

10—20°N, 20—30°S and 40°S, but negative in other regions.

The distributions of annually averaged sea surface temperature, surface (ocean and land) temperature, precipitation rate, soil moisture, sea level pressure are depicted in Fig. 5. It is clear that despite that the distribution pattern of each quantity does not change greatly, the global temperature becomes generally warm due to the incresased CO_2. The warming is about 2—3°C in the extratropical ocean but less than 2°C over the tropical ocean. The rising of SST in the eastern equarorial Pacific leads to the weakening of cold

water tongue (Fig. 5a).

Compared with control run, the notable changes of annual mean surface (ocean and land) temperature are: (i) 20°C isotherm lines extend to 35°N and 40°S from 30°N and 35°S respectively. (ii) the area with SSTs higher than 30°C enlarges. (iii) 0°C isotherm lines extend towards polar regions, meaning that the ice covers over poles decrease (Figs. 5b1 and 5b2). It is also found in Fig. 5b3 that the warming is generally above 2°C in mid- and high-latitudes, the greastest warming is 6°C at northern high latitudes. Warming is generally less than 2°C over tropical oceans and is about 2—4°C over tropical lands.

Unlike the general increase of global surface temperature, there are increase and decrease in the annually averaged precipitation in different areas. The most significant changes occurred in tropics, where precipitation rate clearly decreases over South Africa, Southeast Asia, Malysiya, the central and east parts of the northern Pacific but it increases over India Peninsula, Indian Ocean, Indoniesia Islands and Sahel (Fig. 5c).

Because of CO_2 increase, most of global soil becomes drier except the areas in Australia, Arabian Peninsula, Indian Peninsula, Thailand, Africa between 10°N and 30°N

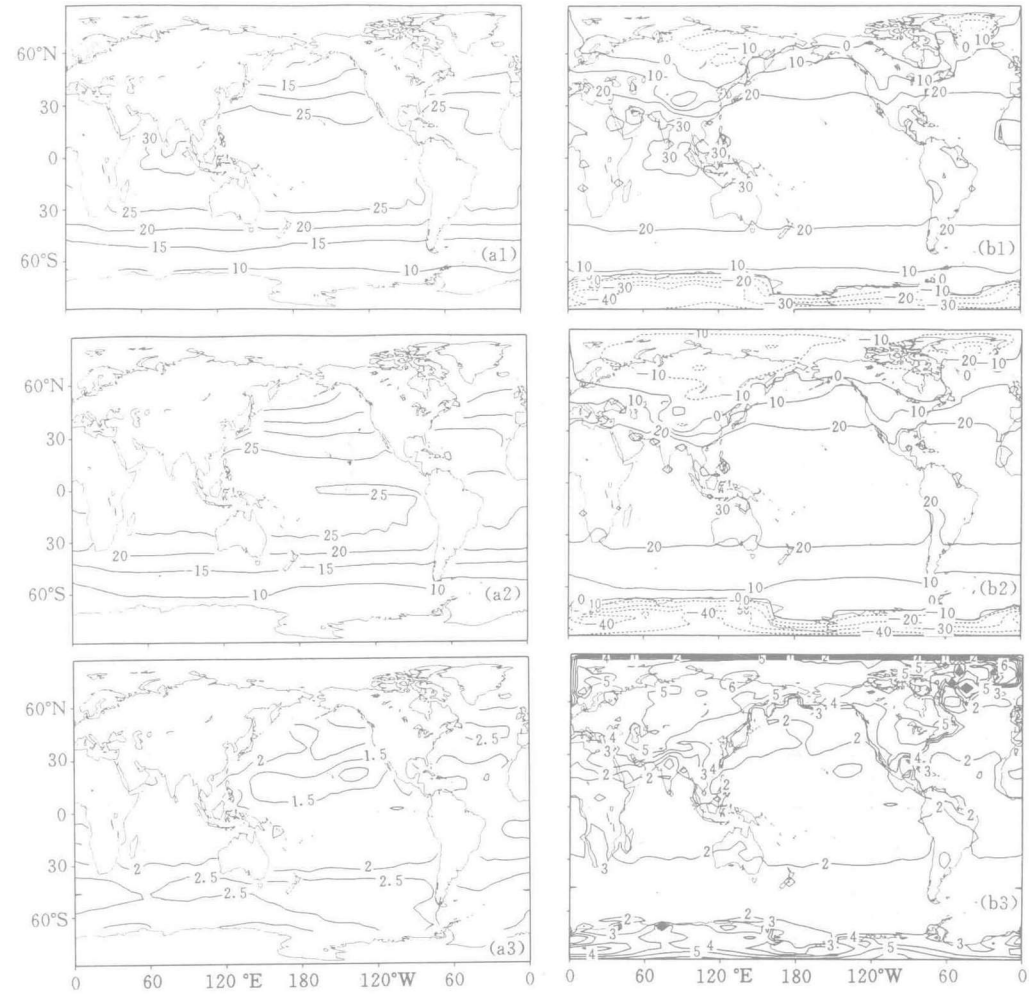

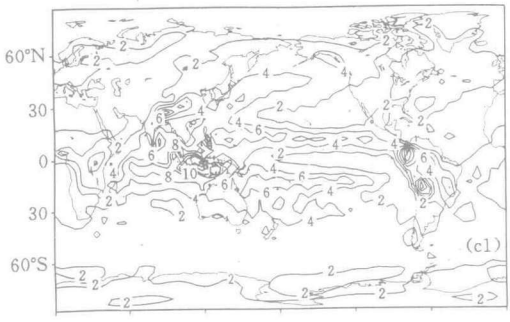
60°N
30
0
30
60°S
(c1)

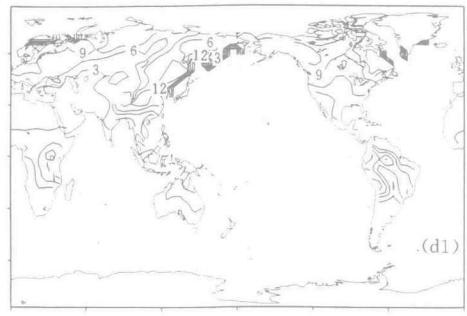
(d1)

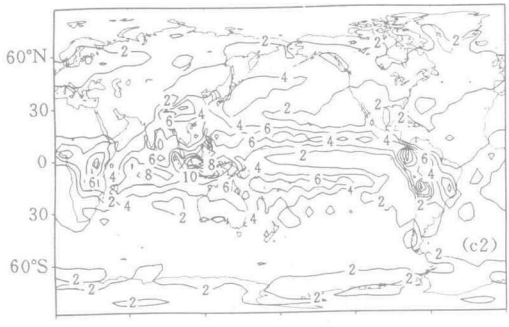
60°N
30
0
30
60°S
(c2)

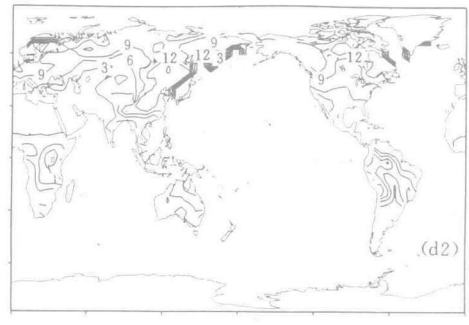
(d2)

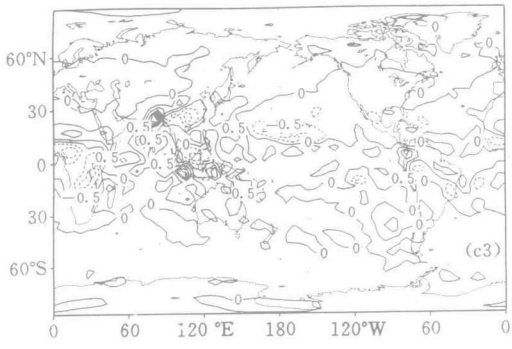
60°N
30
0
30
60°S
(c3)
0 60 120°E 180 120°W 60 0

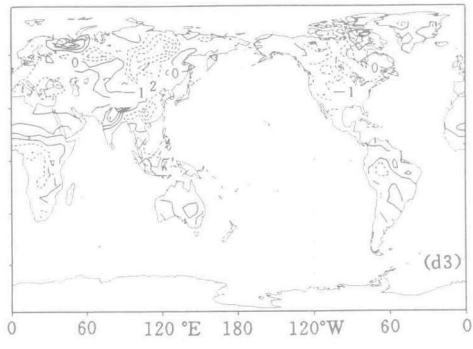
(d3)
0 60 120°E 180 120°W 60 0

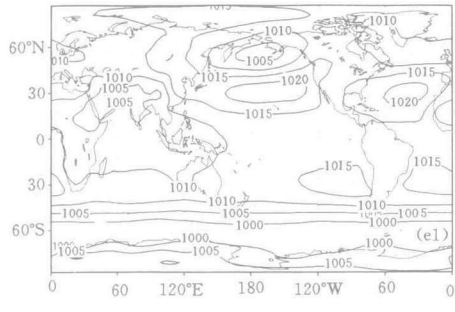
60°N
30
0
30
60°S
(e1)
0 60 120°E 180 120°W 60 0

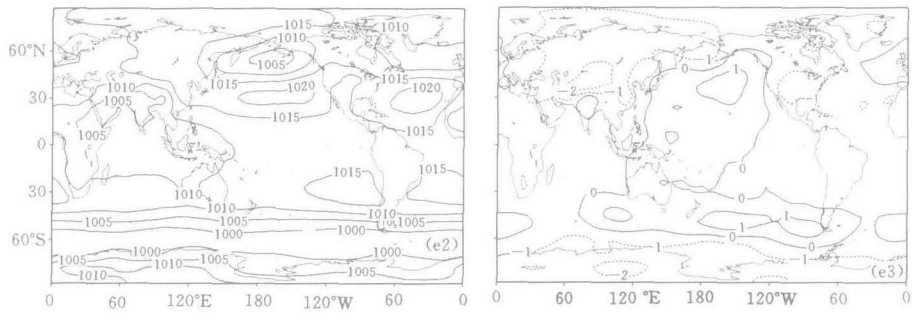

Fig. 5. Horizontal distributions of annual mean sea surface temperature (Fig. 5a), surface (ocean and land) temperature (Fig. 5b), precipitation rate (Fig. 5c), soil moisture (Fig. 5d) and sea level pressure (Fig. 5e). Figures 5a—e1 and 5a—e2 show the distributions of each quantity in $3CO_2$ and $1CO_2$ level respectively: Figs. 5a — e3 show the distributions of $3CO_2$ minus $1CO_2$ differences of each quantity, respectively.

and Northwest Russia, where soil moisture increases (Fig. 5d). It is interesting that increased CO_2 causes precipitation and soil moisture increasing in Sahel (Figs. 5c3 and 5d3). Moreover, annual mean sea level pressure decreases in most of the earth except Australia, most of Pacific Ocean, South Atlantic and South Indian Ocean between 30°S and 60°S (Fig. 5e).

3. *Regional Mean Climate Changes*

The above discussions give the general concepts of climate changes rather than the information of regional or local changes. It is the regional or local change through which the global climate changes can be detected. Therefore, five small areas are selected by referring to IPCC's report in 1990 to analyze and compare the effects of CO_2 increase on the climate in these areas. The five regions are East China (110—120°E, 20—40°N), South Asia (70—100°E, 5—30°N), Australia (115—155°E, 10—40°S), Sahel (10—20°N, 15°W —35°E) and Central North America (35—55°N, 85—105°W). The annual and seasonal (December—January—February for winter and June—July—August for summer) mean changes of TSF, PREC and SM resulting from $3CO_2$ are computed in each directory respectively (Table 3).

As shown in Table 3, the seasonal and annual mean temperatures increase in all regions. The warming in winter is larger than in summer. Different from temperature, precipitation and soil moisture decrease in some places, but increase in other places, and the alteration is larger in summer than in winter. Overall, due to the increased CO_2, the climate changes in East China and Central North America are similar, namely, temperature increases, soil moisture decreases, precipitation increases in winter but decreases in summer and annual mean. The climate changes in South Asia and Australia are similar, that is, temperature and precipitation increase, soil moistures averaged annually and for summer increase. In winter, soil becomes dry in South Asia but becomes wet in Australia. In Sahel of Africa, temperature increases, precipitation and soil moisture averaged annually and for summer increase but decrease for winter.

Table 3. Regional Means of $3CO_2$ minus $1CO_2$ Surface Temperature, Precipitation and Soil Moisture

	Surface temperature (°C)			Precipitation (%)			Soil moisture (%)		
	annual mean	DJF mean	JJA mean	annual mean	DJF mean	JJA mean	annual mean	DJF mean	JJA mean
East China	4.27	5.16	3.38	−4.95	11.37	−18.26	−14.48	−10.46	−19.09
South Asia	1.89	2.41	1.10	20.59	0.10	16.36	16.46	−9.51	23.32
Australia	2.07	2.08	2.13	7.20	7.54	5.63	4.86	5.61	4.14
Sahel	2.23	3.29	1.78	16.62	−13.96	14.95	24.76	−2.07	20.40
Central North America	5.01	5.15	5.05	−4.11	10.95	−17.76	−12.33	−8.56	−21.13

In the IPCC's report in 1990, South Europe, South Asia, Australia, Sahel and Central North America were selected as the five typical regions. The estimations of climate changes in the five regions in 2030 were undertaken under the condition that greenhouse gases were emitted as normal (see Houghton 1994). "The normal emission" is a hypothesis that no strong measure will be adopted to control the emission of CO_2, which is regarded as the most probable conception to the future condition. In view of greatly increasing energy sources as well as destroyed forests and decreasing forest areas, it was predicted that the increasing releases of CO_2 would approximately be 3 times in 2100. The estimated climate changes of South Asia and Central North America in the present paper are consistent with the estimations of IPCC. For example, according to the report of IPCC, the annual warming would be 1—2°C in the South Asia in 2030, there might be little change in precipitation during wintertime (DJF) but the precipitation rate for summer (JJA) might increase 5%—15%. Soil moisture might increase 5%—10% in winter. However, the simulations of climate changes in Australia and Sahel in the present paper differ from IPCC's report. For example, it was estimated by IPCC that temperature would decrease 1—2°C in Australia, but it increases about 2°C in this paper. In fact, even if the several models employed by IPCC did not obtain any consistent estimation to the changes of soil moisture in Australia.

4. *Impact of Increased CO_2 on ENSO-Like Fluctuations*

Another major aspect simulated by CGCM is ENSO-like fluctuation. The occurrence and evolution of ENSO directly or indirectly influence the weather and climate over many countries and regions. For example, it may result in severe disasters such as floods and droughts. Therefore, with the increase of the knowledge on ENSO and greenhouse effect, scientists begin to pay more attention to the probable relationship between ENSO and CO_2-induced global warming. Zebiak and Cane (1991) suggested that the variations of upper ocean layer resulting from increased CO_2 might influence some features of ENSO, such as ENSO's amplitude and frequency. However, Tett's (1995) study indicated that there was no clear change in the interannual variation of SST in the eastern Pacific. Knutson et al.

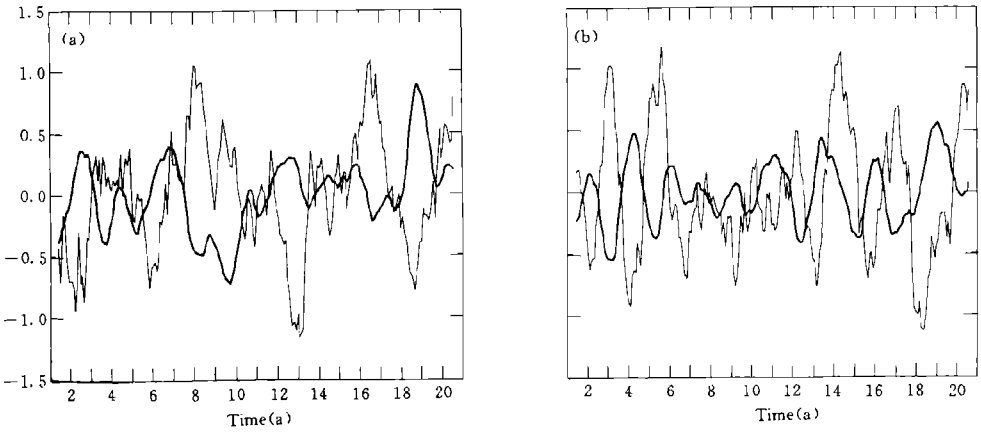

Fig. 6. SST anomalies averaged over Nino3 area in the tropical Pacific Ocean and Southern Oscillation Index (SOI) (with 11-month running average). Nino3 SSTA (think curve) and SOI (thin curve) in $1CO_2$ experiment (a) and $3CO_2$ experiment (b).

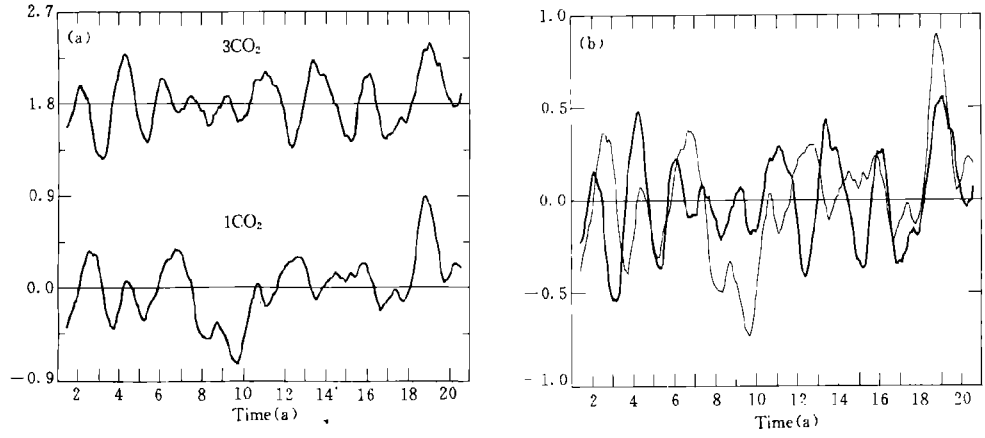

Fig. 7. SST anomalies averaged over the Nino3 area in the tropical eastern Pacific (10°N—10°S, 90—150°W) for the coupled model experiment. (a) $1CO_2$ and $3CO_2$ SST minus the $1CO_2$ long-term mean. (b) $1CO_2$ SST minus $1CO_2$ long-term mean (thin curve) and $3CO_2$ SST minus $3CO_2$ long-term mean (think curve), respectively.

(1997) performed two 1000-year runs in $2CO_2$ and $4CO_2$ levels respectively by using a lower resolution global CGCM and found that the amplitude of model ENSO decreased but the frequency did not change.

The probable impact of increased CO_2 on ENSO is specially analyzed in this section. The sea surface temperature anomaly (SSTA) index in Nino3 area and Southern Oscillation Index (SOI) in $1CO_2$ and $3CO_2$ experiments are presented in Fig. 6. Although the modeling SST and SOI are less than their observational values, there are still significantly out of phase variations in Nino3 Index and SOI in model on the interannual scale. It suggests that ENSO-like fluctuations still exist over the tropical Pacific although CO_2 concentrations increase. Some other modeling studies also indicate that ENSO is a

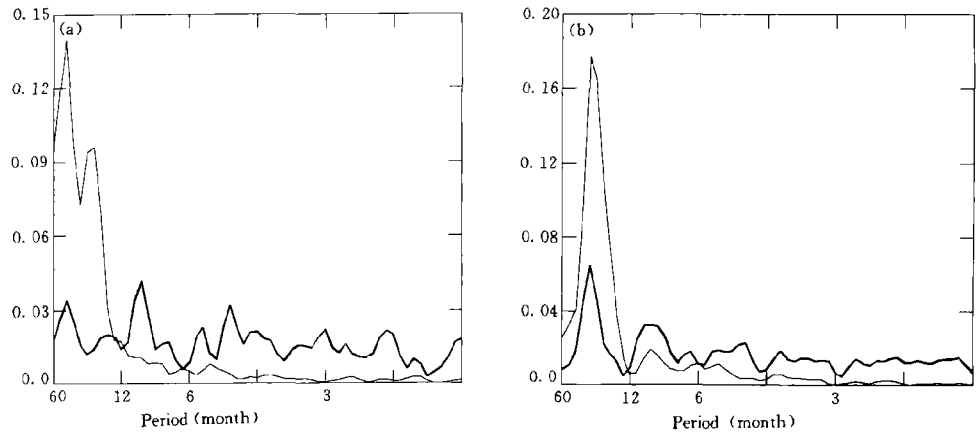

Fig. 8. Power spectra of Nino3 SSTA (thin curve) and SOI (think curve) of the coupled model integration in $1CO_2$ experiment (a) and $3CO_2$ experiment (b). Here the SOI is the normalized pressure difference between the model grid points nearest to Tahiti and Darwin, Australia.

strong feature of earth's climate (see Meehl et al. 1993; Knutson et al. 1997; Tett 1995). With CO_2 increased, the interannual variation of SST over the tropical Pacific Ocean is superimposed upon a mean higher SST. The annual mean SST averaged over Nino3 area approximately rises 1. 8°C (Fig. 7a). The interannual variation of SST in $3CO_2$ level decreases slightly compared with that in $1CO_2$ level (Fig. 7b). We have computed the time-mean zonal contrast in SST along the equator and found that it decreased by about 0. 3°C owing to the CO_2 increase, which might in part attribute to decreased SST variability.

To investigate the impact of CO_2 increase on the frequency of model ENSO, we have computed the power spectra of SSTA in Nino3 area and SOI for the last 20 years (year 22 — 41) of coupled model integration. As shown in Fig. 8, on the interannual time-scale, coinciding with SOI, the SST spectra have two peaks between approximately 20 months and 60 months in $1CO_2$ case but one peak around 30 months in $3CO_2$ case. It suggests that the frequency of the model ENSO changes from 2—5 years in $1CO_2$ to 2. 5 years in $3CO_2$.

V. SUMMARY AND CONCLUDING REMARKS

In the present paper, the simulations in $1CO_2$ and $3CO_2$ experiments with BMRC global coupled atmosphere-ocean-sea ice model are analyzed. The comparisons between $1CO_2$ simulations and observations show that the model used here can describe many notable characteristics of observational climatology very well although there are some errors in the simulations. By comparing $3CO_2$ results with $1CO_2$ results, the probable impacts of CO_2 increase on climate and climate variability have been examined from various points of view, such as global mean, hemispheric mean, zonal mean and geographic distribution, etc.

Because global climate changes are felt through regional or local changes, five small areas are selected to analyze and compare the impacts of CO_2-increase on the climate over the five areas. Some of the results are similar to the report of IPCC (1990), but others are not. Due to the limits of models themselves, such as defects in model resolutions and

model cloud. At present, there are some difficulties and uncertainties to apply models to estimate the variation information of small regions and there are many detailed differences between simulations from various models. Scientists are devoting themselves to improve models in order to improve regional predictability.

Particularly discussed is the issue on whether climate changes concerned with CO_2 increase might influence the interannual variability of SST over tropical Pacific Ocean. It is found that ENSO-like fluctuations in tropical Pacific continually exist over a warmer climate state when CO_2 concentration is increased three-folds. However, the amplitude of the interannual variation of SST in tropical Pacific decreases slightly, the period of ENSO cycle alters from 2—5 years to about 2.5 years.

Of course, current climate variations may not completely be attributed to global warming. It may be caused by other inherent natural variability that has nothing to do with the greenhouse warming, such as the interdecadal climate variability. Nevertheless, the changes of mean climate may modify how climate fluctuations in the tropical Pacific are communicated to the rest of the world. For example, Meehle et al. (1993) found that the associated events in the tropics and subtropics were intensified. Regions that were dry during a warm episode in control run became much drier during a warm episode in increased CO_2 run. Although 41-year integration is not long enough to draw some determined conclusions on the issues that global warming induced by CO_2 increase may change ENSO and its impacts, the present study does explore some questions worthy of thinking deeply and provide the basis for further researches.

The first author wishes to thank Dr. Wang Guomin (BMRC of Australia) for his encouragement and help in preparing this work, and also thank Prof. Ding Yihui and Prof. Zhao Zongci for their helpful comments.

REFERENCES

Gates, W. L., Cook, K. H. and Schlesinger, M. E. (1981). Preliminary analysis of experiments on the climatic effects of increased CO_2 with an atmospheric general circulation model and a climatological ocean. *J. Geophys. Res.*, **86**: 6385—6393.

Houghton, J. (1993). *Global Warming*. The Complete Briefing Lion Publishing Corporation, pp. 240.

Knutson, T. R., Manabe, S. and Gu, D. (1997). Simulated ENSO in a global coupled atmosphere-ocean model: Multidecadal amplitude modulation and CO_2 sensitivity. *J. Climate*, **10**: 131—161.

Li Xiaodong and Zhao Zongci (1996). *Numerical Simulation Study on Climate Changes*. The collections of thesis of studies on the regulations of climate change and its numerical simulation, China Meteor. Press, Beijing, pp. 160—169 (in Chinese).

Meehl, G. A., Branstator, G. W. and Washington, W. M. (1993). Tropical Pacific interannual variability and CO_2 climate change. *J. Climate*, **6**: 42—63.

Schlesinger, M. E. and Zhao Zongci (1989). Seasonal climatic changes induced by doubled CO_2 as simulated by the OSU atmospheric GCM/mixed-layer ocean model. *J. Climate*, **2**: 459—495.

Tett, S. (1995). Simulations of El Nino-Southern Oscillation-like variability in a global AOGCM and its response to CO_2 increase. *J. Climate*, **8**: 1473—1502.

Washington, W. M. and Meehl, G. A. (1986). General circulation model CO_2 sensitivity experiments: Snow-sea ice albedo parameterization and globally averaged surface air temperatuer. *Climatic Change*, **8**: 231—241.

Zebiak, S. E. and Cane, M. A. (1991). Natural climate variability in a coupled model. *Greenhouse Gas-Induced Climatic Change: A Critical Appraisal of Simulations and Observations*. M. E. Schlesinger (Editor). Elsevier Science Ltd., 457—469.